

(K, Na)NbO₃-based lead-free piezoelectric ceramics manufactured by two-step sintering

Xuming Pang, Jinhao Qiu ^{*}, Kongjun Zhu, Jianzhou Du

State Key Laboratory of Mechanics and Control of Mechanical Structures, Nanjing University of Aeronautics and Astronautics, Nanjing 210016, PR China

Received 12 September 2011; received in revised form 7 November 2011; accepted 7 November 2011

Available online 15 November 2011

Abstract

Two-step sintering was applied to manufacture a typical Li- and Ta/Sb-modified alkaline niobate-based lead-free piezoelectric ceramics. The sintering condition dependences of dielectric constants and piezoelectric properties were investigated. Under the optimal condition, dense specimens have an average grain size of approximately 5 μm , and show good dielectric and piezoelectric properties. Significantly, the (K_{0.4425}Na_{0.52}Li_{0.0375})(Nb_{0.8925}Sb_{0.07}Ta_{0.0375})O₃ ceramics sintered under the condition “1130/10/1020/15” show the peak values of the piezoelectric coefficient (d_{33}), electromechanical coupling coefficient (k_p), and dielectric constant (ϵ), which are 281 pC/N, 50% and 1500, respectively, owing to the densest microstructure of typical bimodal grain size distributions. Furthermore, the KNLNST ceramics maintain relatively low dielectric loss over wide temperature ranges. The result indicates that the KNLNST ceramics sintered by two-step sintering exhibit good temperature stability.

© 2011 Elsevier Ltd and Techna Group S.r.l. All rights reserved.

Keywords: A. Sintering; C. Ferroelectric properties; C. Piezoelectric properties

1. Introduction

Perovskite Pb(Zr_xTi_{1-x})O₃-based ceramics are conventional piezoelectric materials widely used in sensor and actuator. However, these ceramics with lead element cause crucial environmental pollution. Therefore, it is important to develop lead-free ceramics with good piezoelectric properties.

Recently, much attention for lead-free piezoelectric ceramics has focused on (K, Na)NbO₃ (KNN)-based ceramics because it is environmental friendly and has good electrical properties [1–15]. However, it was found that sintering of KNN ceramics under atmospheric pressure is difficult. The KNN-based piezoelectric ceramics under atmospheric pressure are difficult in the sintering owing to the volatilization of K and Na in the high temperature sintering which will deviate from the stoichiometry. Many results were only reported in the works based on the pressure sintering such as hot-press (HP) and spark plasma sintering (SPS) [2,12,16–19]. In general, the pressure sintering technique is effective not only to densify the ceramics,

but also to decrease their sintering temperatures which can reduce the volatilization of K and Na; however, such pressure sintering techniques are not best suitable for industrial application due to their low mass productivity. A new method with the advantage of easy-to-use and just only simple equipment is required to manufacture the high properties KNN-based ceramics.

The two-step sintering has been reported for preparing another ceramics. This special sintering process could be seen as the heating rate-controlled sintering and the low-temperature sintering process. It can eliminate the pores and reduce the volatilization of the low-melting-point substances.

In the paper, a typical Li- and Ta/Sb-modified KNN ceramics were prepared by two-step sintering and investigated the dependences of dielectric constant and piezoelectric properties on the two-step sintering conditions.

2. Experimental

K₂CO₃ (99%), Na₂CO₃ (99.8%), Li₂CO₃ (98%), Nb₂O₅ (99.5%), Ta₂O₅ (99.99%), and Sb₂O₃ (99.5%) were used as raw materials to prepare (K_{0.4425}Na_{0.52}Li_{0.0375})(Nb_{0.8925}Sb_{0.07}Ta_{0.0375})O₃ (KNLNST) ceramics by the

^{*} Corresponding author. Tel.: +86 25 84891123; fax: +86 25 84891123.

E-mail address: qiu@nuaa.edu.cn (J. Qiu).

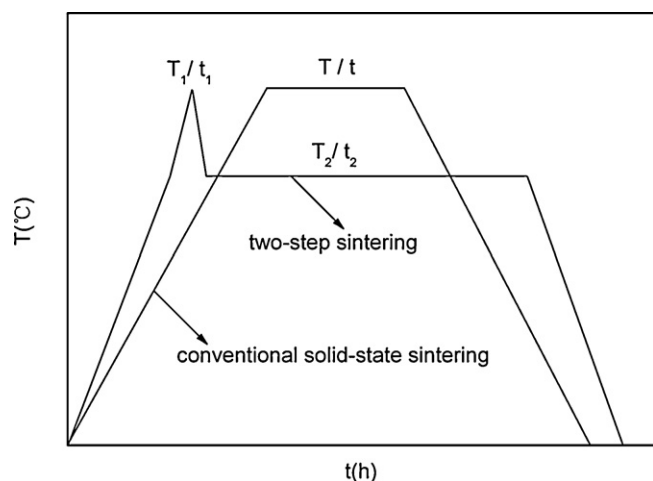


Fig. 1. The sketch of conventional sintering and two-step sintering.

conventional mixed-oxide method. The stoichiometric powders were mixed by ball-milling in ethanol for 5 h, then dried and calcined at 900 °C for 5 h. The calcined powders were mixed with 3 wt% polyvinyl alcohol (PVA) solution, and then uniaxially pressed into pellets with a diameter of 1.5 cm under 300 MPa pressure. After burning out PVA, the KNLNST specimens were fabricated by two-step sintering in sealed alumina crucible. Fig. 1 shows the sintering temperature program schedule. Rate-controlled sintering was programmed from 900 °C to the first sintering temperature T_1 and the heating rate was 10 °C/min. The temperature was held at T_1 for 10 min, rapidly decreased to T_2 at 20 °C/min, and then held at T_2 for the time period t_2 . The sintering temperature of the second stage T_2 was set to be lower than T_1 to densify the samples without/with less grain growth. After that, it follows the furnace cooling. Furthermore, the symbols “ $T_1/t_1/T_2/t_2$ ” are used to indicate two-step sintering, respectively.

The microstructure was observed by using a scanning electron microscope (JSM-5610LV/Noran-Vantage). Powder XRD (D8 Advance) was utilized to identify the crystal structures and the phases. For the measurement of dielectric and piezoelectric properties, silver paste electrodes were formed at the two circular surfaces of the disk-shaped specimens after firing at 700 °C for 10 min. The piezoelectric constant d_{33} was measured using a quasistatic piezoelectric constant testing meter (ZJ-3A, Institute of Acoustics, Chinese Academy of Science, Beijing, China). Dielectric properties as a function of temperature and frequency were measured by an impedance analyzer (HP4294A). Polarization versus electric field hysteresis loops were measured using a ferroelectric tester (TF Analyzer 2000). The measurement of piezoelectric and electromechanical properties was carried out only 24 h after a poling process.

3. Results and discussion

Fig. 2 indicates that all KNLNST ceramics sintered under different conditions exhibit perovskite phases. As shown in Fig. 2, a few impurity phases appear which are several phases

present besides the KNbO_3 perovskite phase based on the phase diagram of the $\text{Nb}_2\text{O}_5\text{--K}_2\text{CO}_3$. With increasing sintering temperature and dwelling time, the diffraction angles shift toward lower ones, such as the samples synthesized below 1120 °C with orthorhombic structure and the samples sintered above 1130 °C with tetragonal structure from Fig. 2(a); therefore, the space distance increased gradually, which could be deduced by Bragg's equation, $2d\sin\theta = \lambda$; here, $\lambda = 1.5416 \text{ \AA}$. With increasing sintering temperature and dwelling time, both Na and K undergo more severe losses, but the extent of K is lesser, which gives rise to a relatively higher K content in individual samples [24]. The eventually increased space distance is attributed to the larger radius (1.33 Å) of K^+ than that of Na^+ (0.97 Å) as well as the relatively higher K content in individual samples. Furthermore, the phase structures of the ceramics sintered by two-step sintering also seem to have relevance to the change of sintering temperature and dwelling time from Fig. 2. The structure transition from orthorhombic to tetragonal is polymorphic phase transition (PPT) which is similar to the MPB behavior as found generally through changing the composition of ceramics [5,20]. As shown in Fig. 2, the ceramics always maintain PPT with the increase of the first-step sintering temperature T_1 from 1110 to 1140 °C, the second-step dwelling time t_2 from 0 to 20 h and the second-step sintering temperature T_2 from 980 to 1040 °C, respectively. This kind of phase structure transition behavior is also attributed to the extent of volatilization of alkali metal ions under high temperature sintering, because many studies confirmed that sodium and potassium volatilize easily during high-temperature sintering [23,24]. As mentioned above, with increasing sintering temperature and dwelling time t_2 , a relatively higher K content in individual samples which gives rise to K/Na rate in individual samples [24]. The structure transition from orthorhombic to tetragonal is similar to the MPB behavior as found generally through changing the K/Na rate of ceramics [23]. The weight changes of the samples are recorded before and after sintering, and the resultant weight loss (the percentage of mass decrease relative to the mass before sintering) value is 0.3% for ceramics sintered under the conditions “1130/10/1020/15”. The weight loss value is lower than the ceramics sintered at 1130 °C by the conventional mixed-oxide method which the weight loss value is 0.5% as our previous study. On the other hand, the structural transition reveals that the real composition of the KNLNST ceramics should be different from the nominal one. So corresponding to the compositional change, the volatilization of alkali metal ions should be related to the phase structure transition behavior, as shown in Fig. 2.

The SEM micrographs of the microstructures of KNLNST ceramics sintered under different conditions are shown in Fig. 3. As shown in Fig. 3(a)–(d), the grains are still within the submicron range even when the samples are sintered at 1110 °C. When T_1 is increased to 1120 °C, the microstructure become denser and the grains grow much larger. And it is easy to distinguish large grains until the sintering temperature T_1 increased to 1130 °C: the grains grew significantly and resulted in a bimodal distribution containing coarse and faceted grains

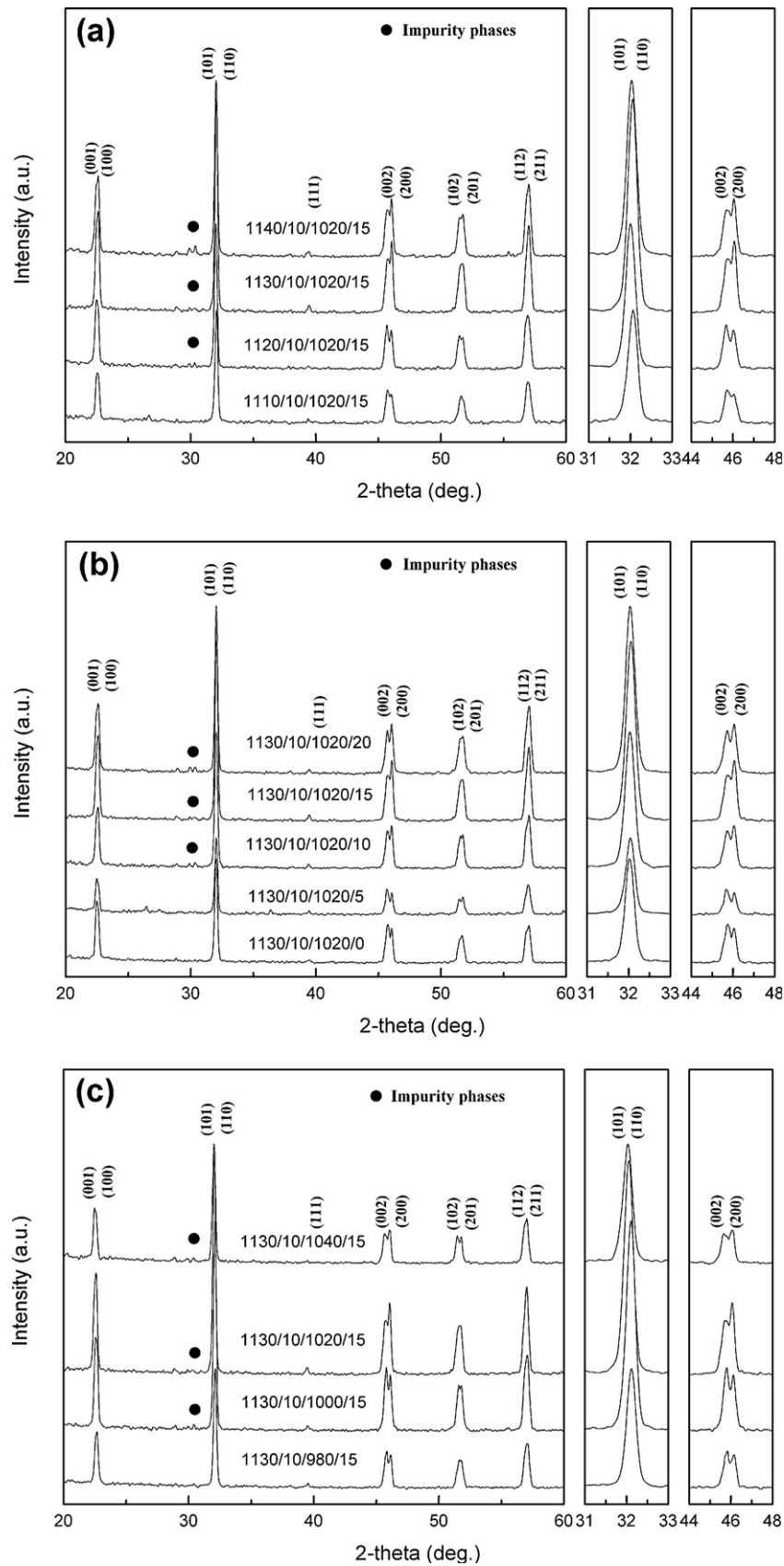


Fig. 2. XRD patterns of the KNLNST ceramics sintered under different conditions, (a) $T_1/10/1020/15$, (b) $1130/10/1020/t_2$, (c) $1130/10/T_2/15$.

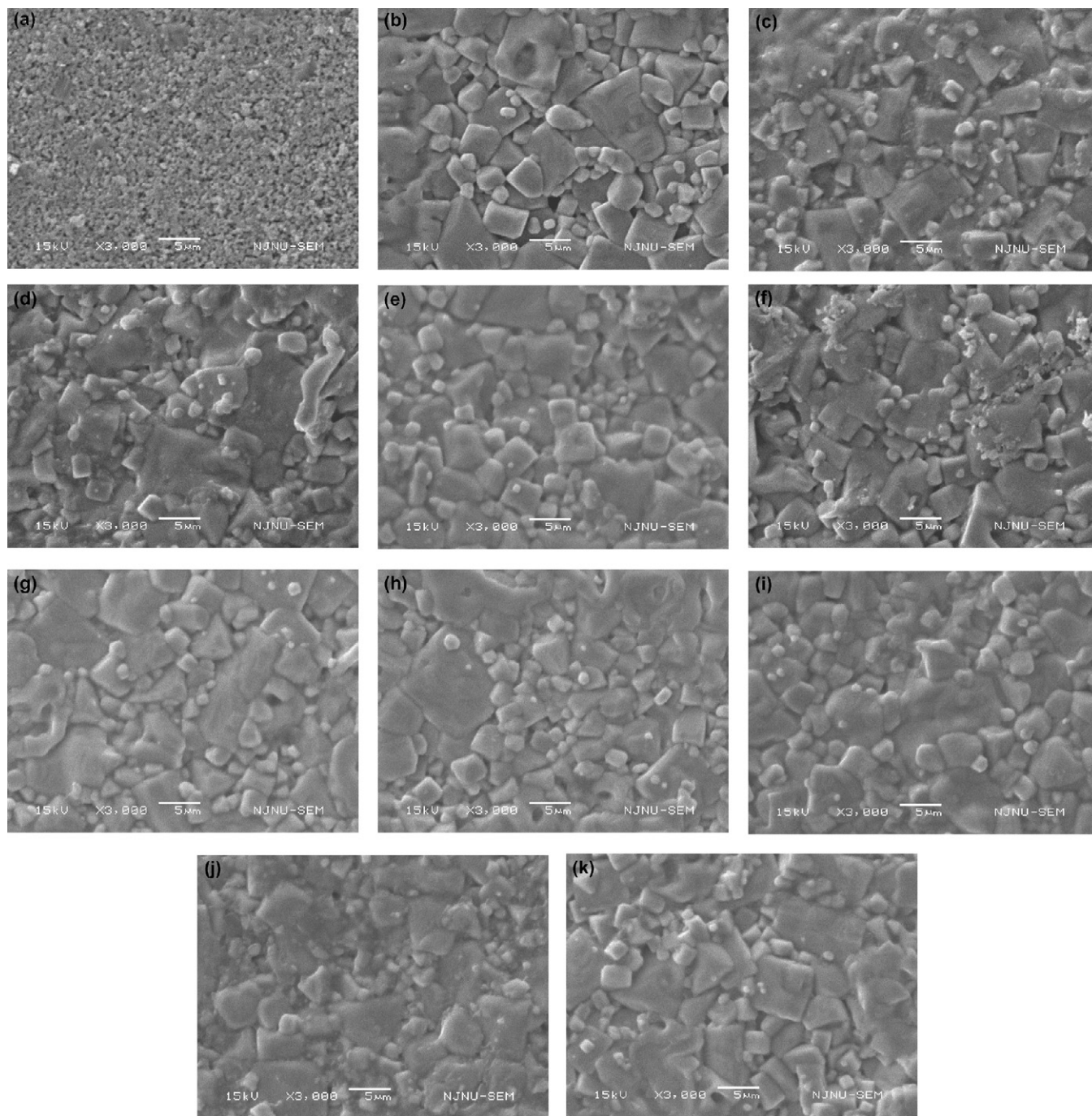


Fig. 3. SEM micrographs of $(K_{0.4425}Na_{0.52}Li_{0.0375})(Nb_{0.8925}Sb_{0.07}Ta_{0.0375})O_3$ ceramics (a) 1110/10/1020/15, (b) 1120/10/1020/15, (c) 1130/10/1020/15, (d) 1140/10/1020/15, (e) 1130/10/1020/0, (f) 1130/10/1020/5, (g) 1130/10/1020/10, (h) 1130/10/1020/20, (i) 1130/10/980/15, (j) 1130/10/1000/15, (k) 1130/10/1040/15.

5 μm in length; many ultra-fine grains are distributed at the boundaries of coarse grains. It can be seen from Fig. 3(d) that some pores exist in the grain boundary of KNLNTS ceramics sintered at 1140 $^{\circ}\text{C}$, and the tetragonality of grain decreases. Because the solidus temperature at of KNN is near 1140 $^{\circ}\text{C}$ [21], it indicates that the liquid phase is formed, which makes sharp corner of gains dissolve. It showed that the grain size is increased as the dwelling time t_2 increased, and all ceramics sintered by two-step sintering exhibit dense microstructures with bimodal grain size distributions from Fig. 3(e)–(h).

Besides, properly increasing dwelling time t_2 can eliminate pores and improve density accordingly. The microstructures of KNLNTS ceramics are dense, as shown in Fig. 3(i)–(k), and the tetragonality of grain enhances with increase of sintering temperature T_2 .

Fig. 4 shows the piezoelectric properties and dielectric properties of the KNLNST ceramics sintered under different conditions. It can be seen that various properties of the ceramics sintered by two-step sintering are strongly dependent on the sintering temperature and dwelling time. The ceramics sintered

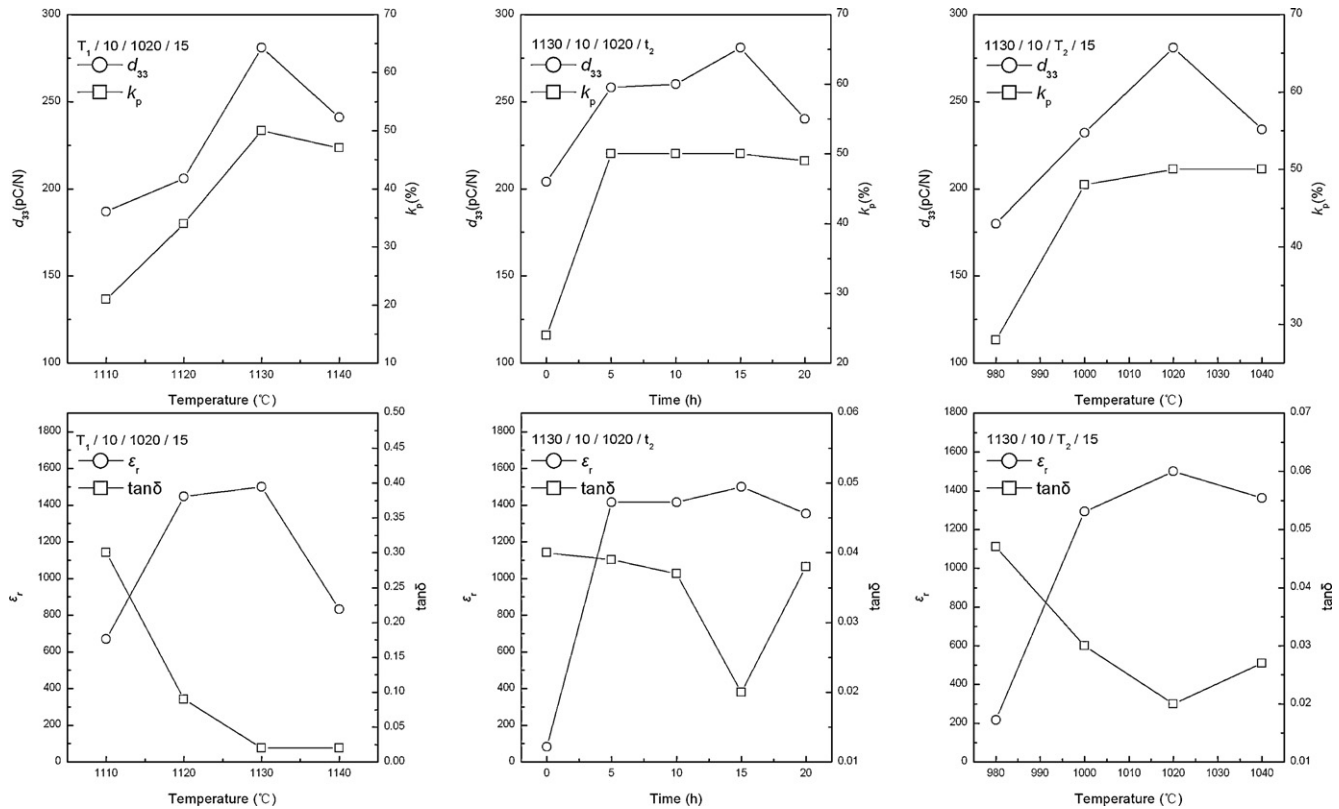


Fig. 4. Dielectric and piezoelectric properties of the ceramics sintered under different conditions.

under the conditions “ $T_1/10/1050/15$ ” and “ $1130/10/T_2/15$ ” reach excellent properties over narrow temperature ranges of T_1 around 1130 °C and T_2 1020 °C, respectively. Furthermore, the properties of the ceramics sintered by two-step sintering can also be improved by the increase of the dwelling time t_2 . As the ceramics sintered under the condition “ $1130/10/1020/t_2$ ”, the d_{33} , k_p , and ϵ_r increase with an increase of the dwelling time t_2 , and the $\tan\delta$ decreases slightly and then rapidly declines to a minimum values around 15 h. Therefore, the piezoelectric constant (d_{33}), electromechanical coupling factor (k_p), and dielectric constant (ϵ_r) in the specimen (1130/10/1020/15) are higher than the others, and the dielectric loss ($\tan\delta$) is smaller. The results show that both density and grain distributed had a strong influence on the final specimens’ properties from Figs. 3 and 4. It is different from the reported that small grain size caused the large piezoelectric constant [22].

Fig. 5 shows the P – E hysteresis loops of the ceramics sintered under different conditions and their corresponding remnant polarizations (P_r) and coercive fields (E_c). As shown in Fig. 5, the P – E hysteresis loops are observed for the ceramics sintered by two-step sintering. However, the sintering temperature (T_1 , T_2) and the dwelling time t_2 have an obvious influence on the ferroelectric properties of the samples sintered by two-step sintering. A round-shaped P – E hysteresis loop is obtained in the sample sintered under the condition “ $1110/10/1020/15$ ”, due to a large leakage current, which suggests that its sintering temperature is not sufficiently high to obtain a dense ceramic. With the increase of sintering temperature (T_1 , T_2) and the dwelling time t_2 , the P – E hysteresis loops of the ceramics

gradually become well-saturated. However, the E_c decreases at the same time, especially for the sample sintered under the condition “ $1130/10/1020/15$ ”. The decrease of coercive field should mainly attribute to the decrease of the amount of defects and the well microstructure under proper sintering temperature (T_1 , T_2) and the dwelling time t_2 . It is well-known that alkali metal ion is volatile and alkali metal ions vacancies will be left at high sintering temperature, which enhance the pinning effects and decrease domain wall mobility correspondingly [23]. Because the samples are mainly sintered at lower temperature T_2 which are only sintered at T_1 for heat preservation for 10 min, these vacancies and the amount of defects are decreased.

Fig. 6 shows the temperature dependence of dielectric constant and loss of KNLNST ceramics sintered under the condition “ $1130/10/1020/15$ ”, which are measured at 10 kHz. As we know, pure KNN ceramics have two phase transitions nearly at 200 °C and 420 °C, corresponding to the orthorhombic–tetragonal (T_{o-t}) and tetragonal–cubic (or Curie temperature T_c) phase transition temperatures, respectively [1]. But a tetragonal–cubic phase transition is observed in the KNLNST ceramics. It suggests that the T_{o-t} shifts downward to below room temperature (beyond the measuring temperature) because of polymorphic phase transition [20], when the KNLNST ceramics sintered by two-step sintering. It means that the room temperature tetragonal phase is obtained for the KNLNST ceramics sintered under the condition “ $1130/10/1020/15$ ”, which corresponds to the XRD results in Fig. 2. Furthermore, the dielectric property and dielectric loss is almost unchanged

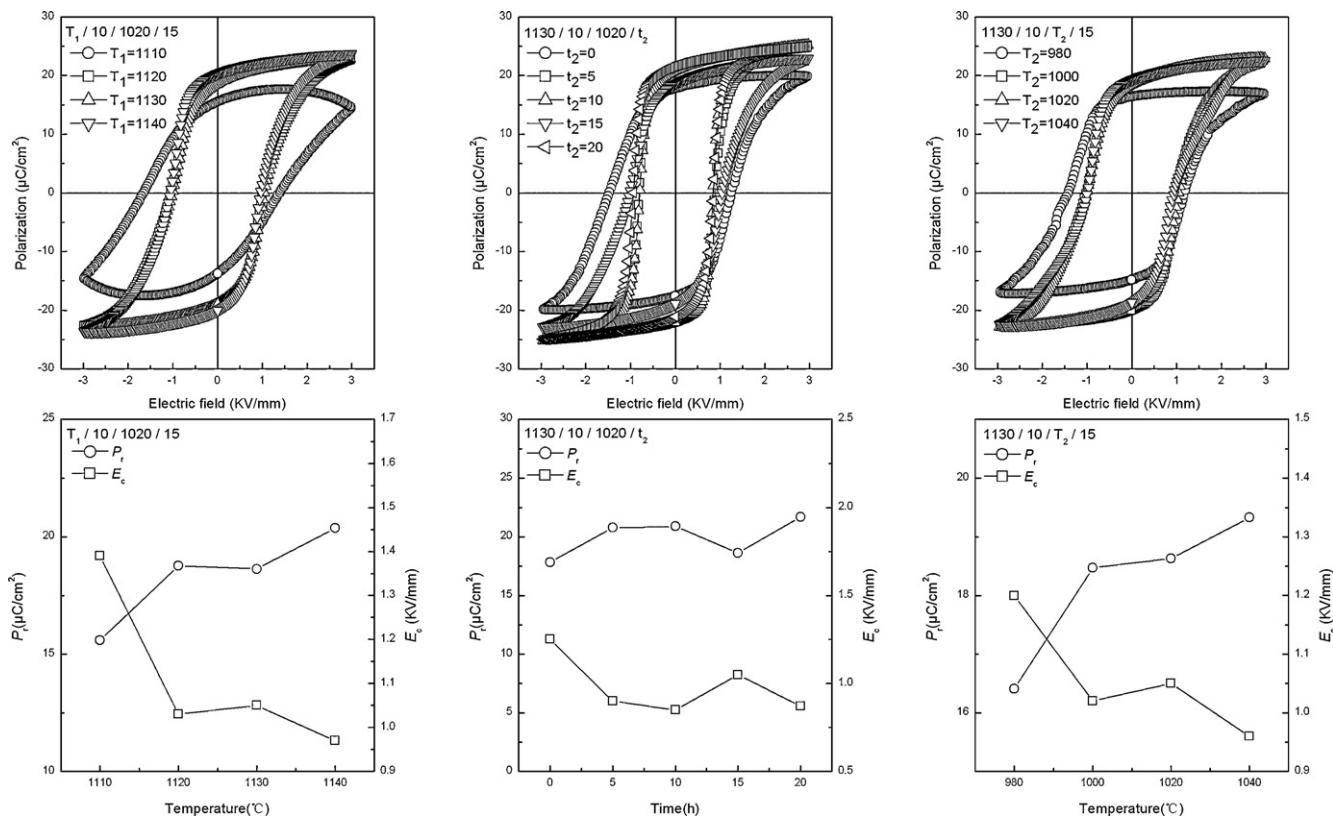


Fig. 5. P - E hysteresis loops of the ceramics sintered under different conditions.

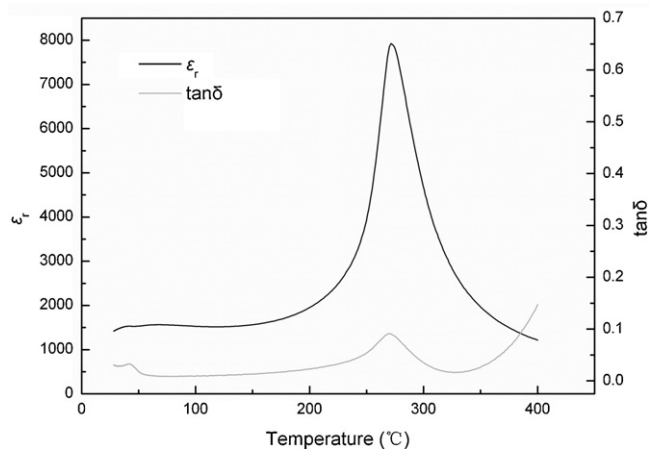


Fig. 6. Temperature dependence of dielectric constant and loss of KNLNST ceramics sintered under the condition "1130/10/1020/15".

when the temperature is below 250 °C. The result indicates that the KNLNST ceramics sintered under the condition "1130/10/1020/15" exhibit good temperature stability.

4. Conclusions

The new sintering process, "two-step sintering" has been developed to improve density and piezoelectric properties of the Li- and Ta/Sb-modified KNN ceramics. The phase structures, microstructures and electrical properties of the

KNN-based ceramics sintered by two-step sintering are obviously dependent on sintering temperature (T_1 , T_2) and the dwelling time t_2 . However, the ceramics sintered under the condition "1130/10/1020/15" exhibit excellent temperature stability over a wide temperature range, which is useful to the application of the KNN-based ceramics.

Acknowledgements

This work was supported by the National Nature Science Foundation of China (NSFC No. 90923029, 51161120326, 51172108), the Natural Science Foundation of Jiangsu Province of China (BK2009020), Program for Changjiang Scholars and Innovative Research Team in University (IRT0968), Program for New Century Excellent Talents in University (NCET-10-0070), A Project Funded by the Priority Academic Program Development of Jiangsu Higher Education Institutions, NUAA Research Fund for Fundamental Research (NJ2010010, NZ2010001), and Funding for Outstanding Doctoral Dissertation in NUAA (No. BCXJ11-02).

References

- [1] L. Egerton, D.M. Dillom, Piezoelectric and dielectric properties of ceramics in the system potassium-sodium niobate, *J. Am. Ceram. Soc.* 42 (1959) 438–442.
- [2] R.E. Jaeger, L. Egerton, Hot pressing of potassium-sodium niobates, *J. Am. Ceram. Soc.* 45 (1962) 209–213.

- [3] Z.S. Ahn, W.A. Schulze, Conventionally sintered $(\text{Na}_{0.5}, \text{K}_{0.5})\text{NbO}_3$ with barium additions, *J. Am. Ceram. Soc.* 70 (1987) 8–21.
- [4] Y. Saito, H. Takao, T. Tani, T. Nonoyama, K. Takatori, T. Hommal, T. Nagaya, M. Nakamura, Lead-free piezoceramics, *Nature* 432 (2004) 84–87.
- [5] Y. Guo, K. Kakimoto, H. Ohsato, Phase transitional behavior and piezoelectric properties of $(\text{Na}_{0.5}\text{K}_{0.5})\text{NbO-LiNbO}_3$ ceramics, *Appl. Phys. Lett.* 85 (2004) 4121–4123.
- [6] M. Matsubara, K. Kikuta, S. Hirano, Piezoelectric properties of $(\text{K}_{0.5}\text{Na}_{0.5})(\text{Nb}_{1-x}\text{Ta}_x)\text{O}_3\text{-K}_{5.4}\text{CuTa}_{10}\text{O}_{29}$ ceramics, *J. Appl. Phys.* 97 (2005) 114105.
- [7] Z.P. Yang, Y.F. Chang, L.L. Wei, Phase transitional behavior and electrical properties of lead-free $(\text{K}_{0.44}\text{Na}_{0.52}\text{Li}_{0.04})(\text{Nb}_{0.96-x}\text{Ta}_x\text{Sb}_{0.04})\text{O}_3$ piezoelectric ceramics, *Appl. Phys. Lett.* 90 (2007) 042911.
- [8] M. Matsubara, T. Yamaguchi, W. Sakamoto, K. Kikuta, T. Yogo, S. Hirano, Processing and piezoelectric properties of lead-free $(\text{K}, \text{Na})(\text{Nb}, \text{Ta})\text{O}_3$ ceramics, *J. Am. Ceram. Soc.* 88 (2005) 190–1196.
- [9] R.Z. Zuo, X.S. Fang, C. Ye, Phase structures and electrical properties of new lead-free $(\text{Na}_{0.5}\text{K}_{0.5})\text{NbO}_3\text{-(Bi}_{0.5}\text{Na}_{0.5})\text{TiO}_3$ ceramics, *Appl. Phys. Lett.* 90 (2007) 092904.
- [10] J.F. Li, K. Wang, B.P. Zhang, L.M. Zhang, Ferroelectric, Piezoelectric properties of fine-grained $\text{Na}_{0.5}\text{K}_{0.5}\text{NbO}_3$ lead-free piezoelectric ceramics prepared by spark plasma sintering, *J. Am. Ceram. Soc.* 89 (2006) 706–709.
- [11] S.J. Zhang, R. Xia, T.R. Shrout, G.Z. Zang, J.F. Wang, Piezoelectric properties in perovskite $0.948(\text{K}_{0.5}\text{Na}_{0.5})\text{NbO}_3\text{-}0.052\text{LiSbO}_3$ lead-free ceramics, *J. Appl. Phys.* 100 (2006) 104108.
- [12] H.L. Du, Z.M. Li, F.S. Tang, S.B. Qu, Z.B. Pei, W.C. Zhou, Preparation, Piezoelectric properties of $(\text{K}_{0.5}\text{Na}_{0.5})\text{NbO}_3$ lead-free piezoelectric ceramics with pressure-less sintering, *Mater. Sci. Eng. B* 131 (2006) 83–87.
- [13] D.M. Lin, K.W. Kwok, K.H. Lam, H.L.W. Chan, Structure and electrical properties of $\text{K}_{0.5}\text{Na}_{0.5}\text{NbO}_3\text{-LiSbO}_3$ lead-free piezoelectric ceramics, *J. Appl. Phys.* 101 (2007) 074111.
- [14] Y.F. Chang, Z.P. Yang, L.L. Wei, Microstructure density and dielectric properties of lead-free $(\text{K}_{0.44}\text{Na}_{0.52}\text{Li}_{0.04})(\text{Nb}_{0.96-x}\text{Ta}_x\text{Sb}_{0.04})\text{O}_3$ piezoelectric ceramics, *J. Am. Ceram. Soc.* 90 (2007) 1656–1658.
- [15] D.M. Lin, K.W. Kwok, H. Tian, H. Wong, L.W. Chan, Phase transitions and electrical properties of $(\text{Na}_{1-x}\text{K}_x)(\text{Nb}_{1-y}\text{Sb}_y)\text{O}_3$ lead-free piezoelectric ceramics with a MnO_2 sintering aid, *J. Am. Ceram. Soc.* 90 (2007) 1458–1463.
- [16] G.H. Haertling, Properties of hot-pressed ferroelectric alkali niobate ceramics, *J. Am. Ceram. Soc.* 50 (1967) 329–330.
- [17] T. Wada, K. Tsuji, T. Saito, Y. Matsuo, Ferroelectric NaNbO_3 ceramics fabricated by spark plasma sintering, *Jpn. J. Appl. Phys.* 42 (2003) 6110–6114.
- [18] R. Wang, R. Xie, T. Sekiya, Y. Shimojo, Fabrication and characterization of potassium-sodium niobate piezoelectric ceramics by spark-plasma-sintering method, *Mater. Res. Bull.* 39 (2004) 1709–1715.
- [19] B.P. Zhang, L.M. Zhang, J.F. Li, H.L. Zhang, S.Z. Jin, SPS sintering of $\text{NaNbO}_3\text{-KNbO}_3$ piezoelectric ceramics, *Mater. Sci. Forum* 475 (2005) 1165–1168.
- [20] Y.J. Dai, X.W. Zhang, G.Y. Zhou, Phase transitional behavior in $\text{K}_{0.5}\text{Na}_{0.5}\text{NbO}_3\text{-LiTaO}_3$ ceramics, *Appl. Phys. Lett.* 90 (2007) 262903.
- [21] X.M. Pang, J.H. Qiu, K.J. Zhu, J. Luo, Study on the sintering mechanism of KNN-based lead-free piezoelectric ceramics, *J. Mater. Sci.* 46 (2011) 2345–2349.
- [22] T. Karaki, K. Yan, M. Adachi, Lead-free piezoelectric ceramics with large dielectric and piezoelectric constants manufactured from BaTiO_3 nanopowder, *Jpn. J. Appl. Phys.* 46 (2007) 97–98.
- [23] Z.Y. Shen, Y.H. Zhen, K. Wang, J.F. Li, Influence of sintering temperature on grain growth and phase structure of compositionally optimized high-performance $\text{Li/Ta-modified (Na, K) NbO}_3$ ceramics, *J. Am. Ceram. Soc.* 92 (2009) 1748–1752.
- [24] P. Zhao, B.P. Zhang, R. Tu, T. Goto, High piezoelectric d_{33} coefficient in Li/Ta/Sb-Co doped lead-free $(\text{Na}, \text{K})\text{NbO}_3$ ceramics sintered at optimal temperature, *J. Am. Ceram. Soc.* 91 (2008) 3078–3081.